Particuology xxx (2016) xxx–xxx

Contents lists available at ScienceDirect

Particuology

journal homepage: www.elsevier.com/locate/partic

Physical vapor transport growth and morphology of Bi_2Se_3 microcrystals

V.V. Atuchin[a,b,c,*], S.V. Borisov[d], T.A. Gavrilova[e], K.A. Kokh[f,g,h], N.V. Kuratieva[d,i], N.V. Pervukhina[d]

[a] Laboratory of Optical Materials and Structures, Institute of Semiconductor Physics, SB RAS, Novosibirsk 630090, Russia
[b] Functional Electronics Laboratory, Tomsk State University, Tomsk 634050, Russia
[c] Laboratory of Semiconductor and Dielectric Materials, Novosibirsk State University, Novosibirsk 630090, Russia
[d] Laboratory of Crystal Chemistry, Institute of Inorganic Chemistry, SB RAS, Novosibirsk 630090, Russia
[e] Laboratory of Nanodiagnostics and Nanolithography, Institute of Semiconductor Physics, SB RAS, Novosibirsk 630090, Russia
[f] Laboratory of Crystal Growth, Institute of Geology and Mineralogy, SB RAS, Novosibirsk 630090, Russia
[g] Geology and Mineralogy Department, Novosibirsk State University, Novosibirsk 630090, Russia
[h] Spintronics Laboratory, Saint Petersburg State University, Saint Petersburg 198504, Russia
[i] Laboratory of Research Methods of Composition and Structure of Functional Materials, Novosibirsk State University, Novosibirsk 630090, Russia

ARTICLE INFO

Article history:
Received 16 August 2015
Received in revised form
24 September 2015
Accepted 7 October 2015
Available online xxx

Keywords:
Bi_2Se_3
Physical vapor transport
Structure
Twin

ABSTRACT

High-quality Bi_2Se_3 microcrystals were grown by the physical vapor transport (PVT) method without using a foreign transport agent. The microplate crystals grown under the optimal temperature gradient are well faceted and have dimensions up to ~200 μm. The growth proceeds by the layer-by-layer mechanism with the formation of flat low-growth rate facets. The phase composition of the grown crystals was identified by the X-ray single crystal structure analysis in space group $R\bar{3}m$, $a = 4.1356(3)$, $c = 28.634(5)$ Å, $Z = 3$ ($R = 0.0147$). The most probable twin planes in the tetradymite structure were evaluated by the pseudo translational sublattice method.

Introduction

Bismuth selenide, Bi_2Se_3, is related to tetradymite-type crystals with general composition A_2B_3 (A = Bi, Sb, As; B = Se, Te) with a trigonal crystal structure (Harker, 1934; Lange, 1939; Semiletov & Pinsker, 1955; Nakajima, 1963). For heavy metals such as Bi and Sb, this structure is observed for pure compounds and solid solutions $(Bi,Sb)_2(Se,Te)_3$, except for the end compound Sb_2Se_3, which has an orthorhombic structure (Voutsas, Papazoglou, Rentzeperis, & Siapkas, 1985). In arsenic compounds, the tetradymite-type modification was observed only for As_2Te_3 (Shu, Jaulmes, & Flahaut, 1988). Conventionally, the trigonal space group $R\bar{3}m$ is accepted for the tetradymite family crystals. However, the structures of Bi_2Te_3 and Sb_2Se_2Te have been resolved in the noncentrosymmetric space group $R3m$ (Atabaeva, Itskevich, Mashkov, Popova, & Vereshchagin, 1968; Andriamihaja, Ibanez, Jumas, Olivier-Fourcade, & Philippot, 1985).

For many years, this selenide has been actively studied because of its pronounced thermoelectric and topological insulator properties (Goltsman, Kudinov, & Smirnov, 1972; Hor et al., 2009; Zhang et al., 2009; Atuchin et al., 2011b; Cava, Ji, Fuccillo, Gibson, & Hor, 2013; Vergniory et al., 2014). The formation of A_2B_3 crystals with a high-quality structure is of prime importance for comparative diagnostics of thin films and nanostructures fabricated by epitaxial and chemical synthesis techniques (Niesner et al., 2012; Norimatsu et al., 2013; Edmonds et al., 2014; Roy et al., 2014; Hsiung, Mou, Lee, & Chen, 2015). One of the most promising methods for this purpose is the physical vapor transport (PVT) method, where the crystalline solid phase is formed by condensation from the vapor phase. The PVT method is well-known and is applicable to the micro- and macrocrystal growth of compounds with volatility that is sufficiently high at increased temperatures. This method has been successfully demonstrated for several volatile oxides, nitrides, and carbides (Sawada & Danielson, 1959; Atuchin et al., 2011a; Chen et al., 2013; Fujimoto et al., 2013; Asakawa et al., 2014; Hartmann,

* Corresponding author at: Institute of Semiconductor Physics, Novosibirsk 630090, Russia. Tel.: +7 383 3308889; fax: +7 383 3332771.
E-mail address: atuchin@isp.nsc.ru (V.V. Atuchin).

http://dx.doi.org/10.1016/j.partic.2015.10.003
1674-2001/

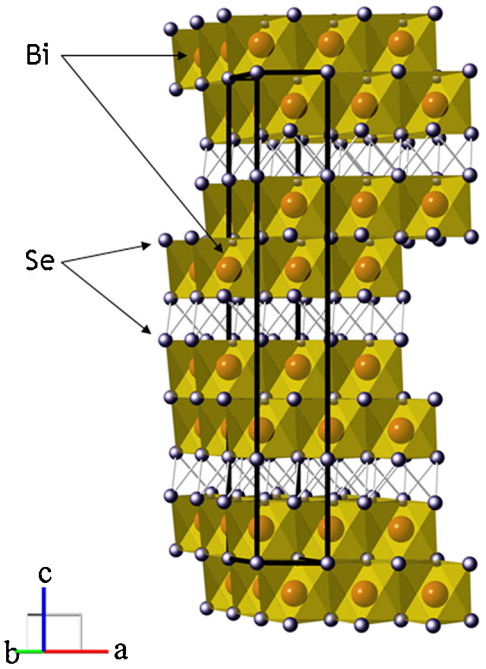

Fig. 1. Crystal structure of Bi_2Se_3. The unit cell is outlined. Lone atoms are omitted for clarity.

Table 1
Crystal data and structure refinement for Bi_2Se_3 in the space group $R\bar{3}m$.

Empirical formula	Bi_2Se_3
Formula weight	654.84
Temperature (K)	293(2)
Wavelength (Å)	0.71073
Crystal system	Trigonal
Space group	$R\bar{3}m$
Unit cell dimensions (Å)	$a = 4.1356(3)$ $c = 28.634(5)$ $\gamma = 120^\circ$
Volume (Å^3)	424.11(9)
Z	3
Density (calculated) (Mg/m^3)	7.692
Absorption coefficient (mm^{-1})	81.296
$F(0\,0\,0)$	804
Crystal size (mm)	$0.10 \times 0.05 \times 0.03$
θ Range for data collection (°)	4.27–32.67
Index ranges	$-6 \le h \le 5$, $-3 \le k \le 6$, $-39 \le l \le 42$
Reflections collected	1737
Independent reflections	243 ($R_{int} = 0.0409$)
Completeness to $\theta = 25.00^\circ$	99.2%
Refinement method	Full-matrix least-squares on F^2
Data/restraints/parameters	243/0/10
Goodness-of-fit on $F2$	1.085
Final R indices ($I > 2\sigma(I)$)	$R_1 = 0.0147$, $wR_2 = 0.0368$
Extinction coefficient	0.00173(14)
Largest difference peak and hole (e/Å3)	1.518 and–1.856

Dittmar, Wollweber, & Bickermann, 2014). Chalcogenide crystals can also be efficiently grown by the PVT method because of high vapor pressure at comparatively low temperatures (Lee et al., 2012; Atuchin et al., 2012; Yang, Kang, Yue, & Yao, 2014; Ma, Cho, & Sung, 2014; Kokh et al., 2014). As a rule, PVT-grown microcrystals are free-standing and well faceted because they contact a substrate or an ampoule wall only at the starting precipitation point. Also, the layer-by-layer growth mode is commonly realized by atom condensation from the vapor phase, which provides high bulk and surface structural quality.

The present study is aimed at the PVT growth of Bi_2Se_3 microcrystals without using a foreign transport agent to exclude the probability of capturing foreign atoms. The crystal structure of Bi_2Se_3, as it was obtained for the polycrystalline material, is shown in Fig. 1 (Nakajima, 1963; Ozawa & Kang, 2004). The lattice is formed by bilayers of face-sharing $BiSe_6$ octahedrons (quintuple). The bilayers are stacked along the c axis by weak van der Waals bonds, with Se–Se distances as long as 351 pm. The bonds can be easily ruptured by mechanical cleavage or a temperature increase. The sublimation kinetics of solid Bi_2Se_3 has been evaluated previously, and preferable evaporation of the Se_2 dimers was found in the temperature range of $T = 800$–900 K (Cafaro, Bardi, & Piacente, 1984).

Experimental

High-purity (4 N) elementary Bi and Se were used for the charge preparation (Shevtsov, 2011; Chanysheva, Podolyanchenko, & Shelpakova, 1997). The growth experiment was performed in a fused 300-mm-long silica ampoule 15 mm in diameter, initially etched with HF-HNO_3 acid mix and rinsed with bidistilled water. The element charge of 15 g was weighed in the stoichiometric composition of Bi:Se = 2:3 and fused in the ampoule sealed at a residual pressure of $\sim 10^{-4}$ bar. The sealed ampoule was placed in a single-zone horizontal furnace to obtain the synthesized Bi_2Se_3 compound using a technique described elsewhere (Kokh, Andreev, Svetlichnyi, Lanskii, & Kokh, 2011; Atuchin et al., 2013a; Atuchin, Borisov, Magarill, & Pervukhina, 2013b). After synthesis, the ampoule was inclined so that the melt was located in the high-temperature part of the ampoule, while the opposite end was at a temperature below the melting point of Bi_2Se_3 (978 K) (Okamoto, 1994). The Bi_2Se_3 melt was taken to be a vapor source because, earlier, it was reported that, at comparatively low source temperatures, i.e., $T = 800$–900 K, selenium dimers dominate in the vapor phase (Cafaro et al., 1984). Additionally, the equilibrium vapor pressure over solid Bi_2Se_3 was considered to be comparatively low. Earlier, for the related compound Sb_2Te_3, it was shown that vaporization from the crystal surface appeared with molecular forms of Sb_2Te_2, Te_2, and SbTe that seemed to be not optimal (Piacente, Scardala, & Ferro, 1992). Using Bi_2Se_3 melt as a source increases the total vapor pressure and provides parallel evaporation of Bi and Se, supposedly in atomic forms. The precipitation of microcrystals occurred at the opposite part of the ampoule, located in the cold zone (~950 K). The growth experiment lasted for ~120 h. Then, the furnace was slowly cooled down to room temperature at the rate of 20 K/h and the ampoule was cracked to obtain silica pieces covered with Bi_2Se_3 microcrystals. The resulting PVT-grown dark plate-like crystals were up to 200 μm in size.

The micromorphology of the crystals formed on the ampoule walls was observed by scanning electron microscopy (SEM) using a LEO 1430 device (Zeiss, Germany). X-ray intensity data were collected from the selected microcrystals on a Bruker X8Apex CCD diffractometer using standard techniques (ω- and φ-scans of narrow frames) and corrected for absorption effects (SADABS) (Bruker AXS Inc., 2004). The structure was solved by direct methods (Burla et al., 2005) and refined by full-matrix least-squares on F^2 using the SHELX97 program set (Sheldrick, 1998). Crystallographic data and details of single crystal diffraction experiments for the compound Bi_2Se_3 are given in Table 1. All atoms were refined anisotropically. Atomic coordinates and equivalent isotropic displacement parameters for Bi_2Se_3, as carried out in the conventional space group $R\bar{3}m$, are given in Table 1S (Supplement). The related bond lengths are given in Table 2S (Supplement).

Results and discussion

The SEM images of grown crystals are shown in Fig. 2, 1S, and 2S. Individual well-faceted plate-like microcrystals (Fig. 2) and

Please cite this article in press as: Atuchin, V. V., et al. Physical vapor transport growth and morphology of Bi_2Se_3 microcrystals. *Particuology* (2016), http://dx.doi.org/10.1016/j.partic.2015.10.003

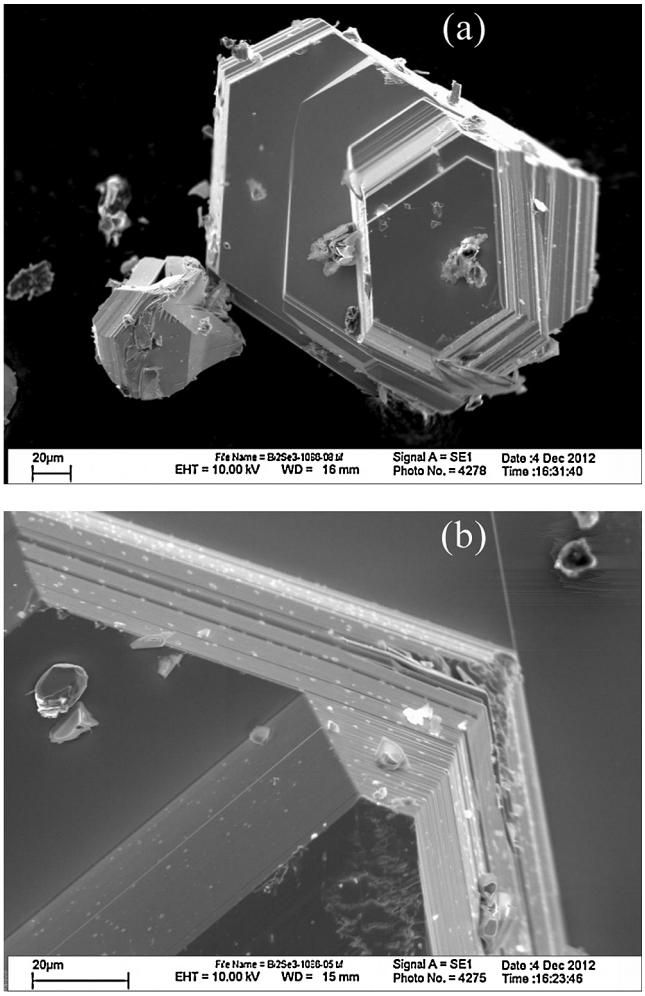

Fig. 2. SEM images of (a) Bi_2Se_3 microplate crystal and (b) the growth of terrace edges.

semispherical particles (Figs. 1S and 2S) were found on the internal surface of the dissected silica ampoule. As a rule, the crystals were poorly clamped to the ampoule wall with a small-area bottom spot and they can be easily separated without damage. The selected plate crystals were as large as 50–200 μm in size. As shown in Fig. 2, the growth proceeds by the layer-by-layer mechanism with the formation of flat low-growth rate facets. This is typical growth behavior for layer-structured crystals with high volatility (Atuchin et al., 2011a, 2012; Atuchin et al., 2013a; Atuchin et al., 2013b; Asakawa et al., 2014; Lee et al., 2012; Yang et al., 2014; Ma et al., 2014; Kokh et al., 2014). The phase composition of the grown crystals was identified by X-ray single crystal structure analysis carried out in the space group $R\bar{3}m$, $a = 4.1356(3)$ Å, $c = 28.634(5)$ Å, $Z = 3$ ($R = 0.0147$) for selected plate microcrystals without macroscopic twinning. The structural parameters are similar to those earlier obtained for Bi_2Se_3 (Nakajima, 1963). Practically equivalent structure solutions can be obtained in the space groups $R\bar{3}$, $R3$, $R3m$, $R32$, and $R\bar{3}m$, and the real symmetry of the Bi_2Se_3 structure can be elucidated only with the help of physical property measurements (Atuchin, Kidyarov, & Pervukhina, 2004; Kidyarov & Atuchin, 2007; Kidyarov, Atuchin, & Pervukhina, 2010). As an example for comparison, the crystallographic parameters obtained in the space group $R\bar{3}$ are shown in Tables 3S–5S.

A large part of the microcrystals was twinned, and the representative SEM images are shown in Figs. 1S and 2S. The large, flat surfaces visible on the particle bottom in Fig. 2S(a) and on the particle top in Fig. 2S(b) are the contact spots with the ampoule wall. Because of the large number of twin boundaries and small terraces, the growth rate of the twinned crystals is much greater than that of single crystal plates. Then, with increasing time, the crystal growth is swiftly finished by the fractal process that appeared for low-growth rate facets, and the semispherical particles, as shown in Fig. 2S(b), should be covered by the very small (0 0 1) facets.

Table 2
The atomic planes ($h\,k\,l$) with the highest atom occupancy (the most intensive reflections F_{hkl}), interplane distances d_{hkl}, and indices ($h\,k\,l$)$_c$ in the sublattice of Bi_2Se_3.

2θ (°)	d_{hkl}	F_{hkl}	$h\,k\,l$	$(h\,k\,l)_c$
29.4	3.04	685	0 1 5	1 0 0
40.3	2.24	607	$\bar{1}$ 1 1 0	1 1 0
43.7	2.07	629	$\bar{1}$ 2 0	1 0 $\bar{1}$
47.6	1.91	540	0 0 $\bar{15}$	1 1 1
53.6	1.71	581	$\bar{2}$ 2 5	1 1 $\bar{1}$
61.0	1.52	532	0 2 1 0	2 0 0
66.6	1.40	481	$\bar{1}$ 2 1 5	2 1 0
71.6	1.32	522	$\bar{1}$ 3 5	2 0 $\bar{1}$
78.0	1.22	483	$\bar{2}$ 3 1 0	2 1 $\bar{1}$
80.4	1.19	504	0 3 0	$\bar{1}$ 2 $\bar{1}$ $\bar{1}$

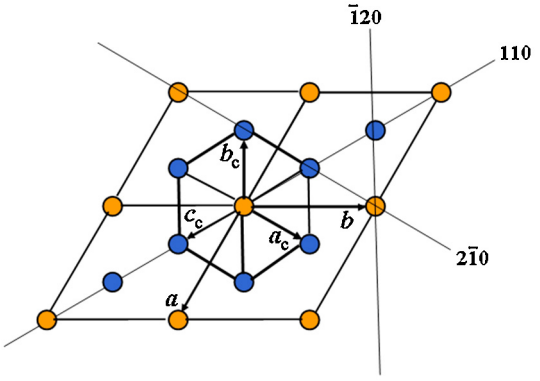

Fig. 3. Relationship of R-cell parameters of Bi_2Se_3 to subcell parameters a_c, b_c, and c_c.

It is useful to determine the possible twin planes in the Bi_2Se_3 structure. The trigonal structure shown in Fig. 1 was analyzed by the pseudotranslational sublattice method—the crystallographic method (Borisov, Magarill, & Pervukhina, 2011). This method has been used for detailed observation of many specific crystal structures (Atuchin, Borisov, Magarill, & Pervukhina, 2011; Atuchin et al., 2013a; Atuchin et al., 2013b; Borisov, Magarill, & Pervukhina, 2012; Borisov, Magarill, & Pervukhina, 2014). To elucidate the premises of the Bi_2Se_3 lattice for twinning, the theoretical diffraction pattern was calculated and the most intensive reflections ($F_{hkl} > 450$ electronic units) were revealed, as shown in Table 2. The intensive reflections relate to atomic plane sets with the highest atom occupancy. Three equivalent plane sets, i.e., (0 1 5), ($\bar{1}$ 0 5), and (1 $\bar{1}$ 5), aligned by the third-order symmetry axis, were considered as coordinate planes of the pseudotranslational lattice ordering the atom positions. The subcell parameters were calculated using the relations $a_c = 1/3a + 2/3b + 1/15c = 3.06$ Å, $b_c = -2/3a - 1/3b + 1/15c = 3.06$ Å, $c_c = 1/3a - 1/3b + 1/15c = 3.06$ Å, and $\alpha_c = \beta_c = \gamma_c = 85.13°$ (Gromilov, Bykova, & Borisov, 2011). Thus, the trigonal subcell is similar to the primitive cubic one, as shown in Fig. 3. The subcell holds 15 sites in a unit cell, and all the sites contain atoms (9Se + 6Bi). In the calculated diffraction pattern, all strong reflections are attributed to the crystallographic planes of this trigonal sublattice, which verifies their domination of the Bi_2Se_3 structure ordering. As shown in Table 2, the intensity of reflection from plane ($\bar{1}$ 2 0) ranks next to that from plane (0 1 5). The atom arrangement in an identical plane (1 1 0) is shown in Fig. 4. The

Please cite this article in press as: Atuchin, V. V., et al. Physical vapor transport growth and morphology of Bi_2Se_3 microcrystals. *Particuology* (2016), http://dx.doi.org/10.1016/j.partic.2015.10.003

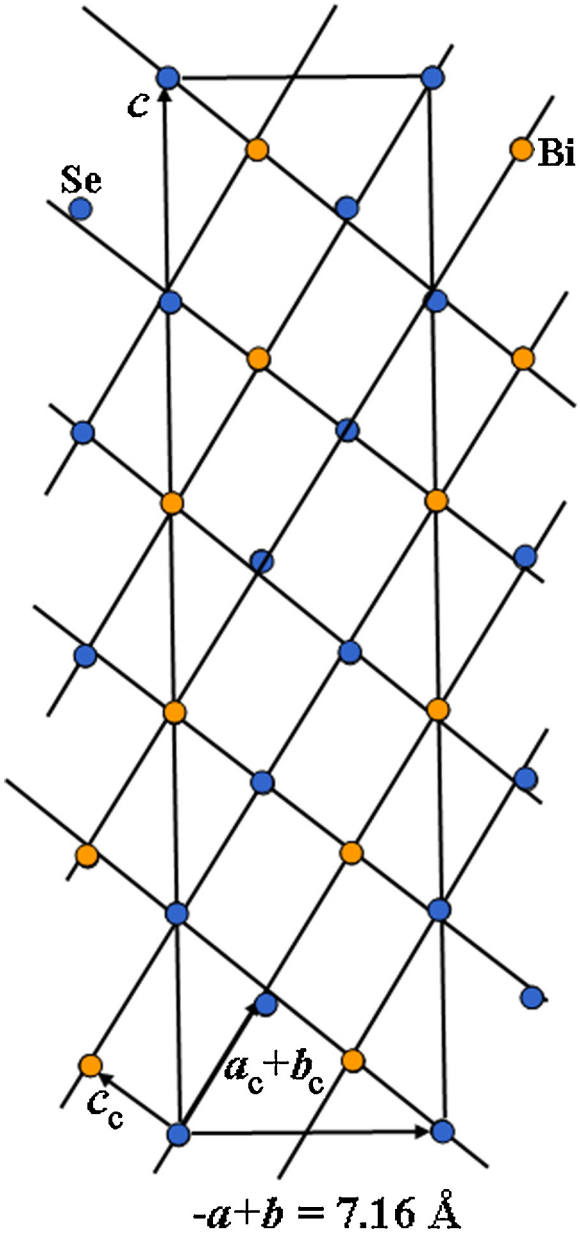

Fig. 4. Positions of Bi and Se in plane (1 1 0). The cubic subcell translations are shown.

perfectly flat and very dense atom nets in the equivalent planes ($\bar{1}$ 2 0), (1 1 0), and (2 $\bar{1}$ 0) may serve as the twinning planes. The planes are parallel to axis ***c*** and intersect at angles of 60°. The twinning process may be the source of druse formation, as shown in Figs. 1S and 2S(a). Also, possible nanolevel twinning of the Bi_2Se_3 crystal during growth and cooling may be a factor complicating crystal symmetry determination.

Conclusions

Well-faceted plate-like microcrystals of Bi_2Se_3 up to ~200 μm in size can be grown by condensation from self-vapor in a sealed silica ampoule under the optimal thermal gradient. The crystals are of high structural quality and have a developed (0 0 1) surface suitable for physical parameter measurements, as verified by single crystal structure analysis. The PVT-grown Bi_2Se_3 microcrystals can be used as a reference in the comparative observation of Bi_3Se_3-based films and nanostructures, including solid solution systems. As shown by the pseudotranslational sublattice method, the tetradymite structure possesses many possible twin planes, and twinning can greatly decrease crystal structural quality.

Acknowledgements

This study was partly supported the Russian Foundation for Basis Research (Grant 14-08-3110). Partial support from Saint Petersburg State University (project 11.50.202.2015) is acknowledged. The studies were carried out using the instrumental equipment of CCU "Nanostructures". This work was supported in part by the Ministry of Education and Science of the Russian Federation (project ID RFMEFI62114X0004) and RSCF (project No. 14-22-00143). This study (research grant No. 8.2.06.2015) was partly supported by the Tomsk State University Academician D.I. Mendeleev Fund Program in 2015. V.V.A. gratefully acknowledges the Ministry of Education and Science of the Russian Federation for the financial support.

Appendix A. Supplementary data

Supplementary data associated with this article can be found, in the online version, at http://dx.doi.org/10.1016/j.partic.2015.10.003.

References

Andriamihaja, A., Ibanez, A., Jumas, J. C., Olivier-Fourcade, J., & Philippot, E. (1985). Evolution structurale de la solution solide $Sb_2Te_{3-x}Se_x$ ($0 \le x \le 2$) dans le système Sb_2Te_3-Sb_2Se_3. *Revue de Chimie Minérale*, *22*(3), 357–368.

Asakawa, H., Sazaki, G., Yokoyama, E., Nagashima, K., Nakatsubo, S., & Furukawa, Y. (2014). Roles of surface/volume diffusion in the growth kinetics of elementary spiral steps on ice basal faces grown from water vapor. *Crystal Growth & Design*, *14*(7), 3210–3220.

Atabaeva, É. Y., Itskevich, E. S., Mashkov, S. A., Popova, S. V., & Vereshchagin, L. F. (1968). Polymorphism of bismuth telluride at high pressures and temperatures. *Fizika Tverdogo Tela*, *10*, 62–65.

Atuchin, V. V., Beisel, N. F., Kokh, K. A., Kruchinin, V. N., Korolkov, I. V., Pokrovsky, L. D., et al. (2013). Growth and microstructure of heterogeneous crystal GaSe: InS. *CrystEngComm*, *15*(7), 1365–1369.

Atuchin, V. V., Borisov, S. V., Magarill, S. A., & Pervukhina, N. V. (2011). Crystal structural premises to epitaxial contacts for a series of mercury-containing compounds. *Journal of Crystal Growth*, *318*(1), 1125–1128.

Atuchin, V. V., Borisov, S. V., Magarill, S. A., & Pervukhina, N. V. (2013). Sphalerite framework in polar sulfides. *Journal of Chemical Crystallography*, *43*(9), 488–492.

Atuchin, V. V., Gavrilova, T. A., Grigorieva, T. I., Kuratieva, N. V., Okotrub, K. A., Pervukhina, N. V., et al. (2011). Sublimation growth and vibrational microspectrometry of α-MoO_3 single crystals. *Journal of Crystal Growth*, *318*(1), 987–990.

Atuchin, V. V., Golyashov, V. A., Kokh, K. A., Korolkov, I. V., Kozhukhov, A. S., Kruchinin, V. N., et al. (2011). Formation of inert Bi_2Se_3 (0 0 0 1) cleaved surface. *Crystal Growth & Design*, *11*(12), 5507–5514.

Atuchin, V. V., Gavrilova, T. A., Kokh, K. A., Kuratieva, N. V., Pervukhina, N. V., & Surovtsev, N. V. (2012). Structural and vibrational properties of PVT grown Bi_2Te_3 microcrystals. *Solid State Communications*, *152*(13), 1119–1122.

Atuchin, V. V., Kidyarov, B. I., & Pervukhina, N. V. (2004). Phenomenological modeling and design of new acentric crystals for optoelectronics. *Computational Materials Science*, *30*(3), 411–418.

Borisov, S. V., Magarill, S. A., & Pervukhina, N. V. (2011). Analysis of atomic structures as the development of Belov's lattice crystallography. *Crystallography Reports*, *56*(6), 935–940.

Borisov, S. V., Magarill, S. A., & Pervukhina, N. V. (2012). Crystallographic analysis of microtwin structures of sulfides: The case study of lillianite and heyrovskyite. *Journal of Structural Chemistry*, *53*(4), 734–739.

Borisov, S. V., Magarill, S. A., & Pervukhina, N. V. (2014). Structure of $Tl_{18}Pb_2Ti_7S_{25}$ as a masterpiece of crystallographic symmetry. *Crystallography Reports*, *59*(6), 843–846.

Bruker AXS Inc. (2004). *Bruker advanced X-ray solutions. APEX2 (version 1.08), SAINT (version 7.03), and SADABS (version 2.11)*. Madison, Wisconsin, USA: Bruker AXS Inc.

Burla, M. C., Caliandro, R., Camalli, M., Carrozzini, B., Cascarano, G. L., De Caro, L., et al. (2005). SIR2004: An improved tool for crystal structure determination and refinement. *Journal of Applied Crystallography*, *38*(2), 381–388.

Cafaro, M. L., Bardi, G., & Piacente, V. (1984). Vaporization study of solid bismuth selenide (Bi_2Se_3). *Journal of Chemical and Engineering Data*, *29*(1), 78–80.

Cava, R. J., Ji, H., Fuccillo, M. K., Gibson, Q. D., & Hor, Y. S. (2013). Crystal structure and chemistry of topological insulators. *Journal of Materials Chemistry C*, *1*(19), 3176–3189.

Please cite this article in press as: Atuchin, V. V., et al. Physical vapor transport growth and morphology of Bi_2Se_3 microcrystals. *Particuology* (2016), http://dx.doi.org/10.1016/j.partic.2015.10.003

Chanysheva, T. A., Podolyanchenko, S. N., & Shelpakova, I. R. (1997). Analysis of high-purity selenium with concentration of impurities by matrix distillation. *Journal of Analytical Chemistry*, *52*(4), 368–372.

Chen, R. S., Wang, W. C., Chan, C. H., Hsu, H. P., Tien, L. C., & Chen, Y. J. (2013). Photoconductivities in monocrystalline layered V_2O_5 nanowires grown by physical vapor deposition. *Nanoscale Research Letters*, *8*(1), 443.

Edmonds, M. T., Hellerstedt, J. T., Tadich, A., Schenk, A., O'Donnell, K. M., Tosado, J., et al. (2014). Stability and surface reconstruction of topological insulator Bi_2Se_3 on exposure to atmosphere. *The Journal of Physical Chemistry C*, *118*(35), 20413–20419.

Fujimoto, T., Ohtani, N., Tsuge, H., Katsuno, M., Sato, S., Nakabayashi, M., et al. (2013). A thermodynamic mechanism for PVT growth phenomena of SiC single crystals. *ECS Journal of Solid State Science and Technology*, *2*(8), N3018–N3021.

Goltzman, B. M., Kudinov, V. A., & Smirnov, I. A. (1972). *Semiconductor thermoelectric materials on the basis of Bi_2Te_3*. Moscow: Nauka.

Gromilov, S. A., Bykova, E. A., & Borisov, S. V. (2011). Algorithms, software, and examples of pseudotranslational sublattice analysis for crystal structures. *Crystallography Reports*, *56*(6), 947–952.

Harker, D. (1934). The crystal structure of the mineral tetradymite, Bi_2Te_2S. *Zeitschrift für Kristallographie-Crystalline Materials*, *89*(1), 175–181.

Hartmann, C., Dittmar, A., Wollweber, J., & Bickermann, M. (2014). Bulk AlN growth by physical vapour transport. *Semiconductor Science and Technology*, *29*(8), 084002.

Hor, Y. S., Richardella, A., Roushan, P., Xia, Y., Checkelsky, J. G., Yazdani, A., et al. (2009). p-Type Bi_2Se_3 for topological insulator and low-temperature thermoelectric applications. *Physical Review B*, *79*(19), 195208.

Hsiung, T. C., Mou, C. Y., Lee, T. K., & Chen, Y. Y. (2015). Surface-dominated transport and enhanced thermoelectric figure of merit in topological insulator $Bi_{1.5}Sb_{0.5}Te_{1.7}Se_{1.3}$. *Nanoscale*, *7*(2), 518–523.

Kidyarov, B. I., & Atuchin, V. V. (2007). Universal crystal classification system point symmetry–physical property. *Ferroelectrics*, *360*(1), 96–99.

Kidyarov, B. I., Atuchin, V. V., & Pervukhina, N. V. (2010). Crystal structure–property relationship as a factor in the refinement of structural physical data. *Journal of Structural Chemistry*, *51*(6), 1119–1125.

Kokh, K. A., Andreev, Y. M., Svetlichnyi, V. A., Lanskii, G. V., & Kokh, A. E. (2011). Growth of GaSe and GaS single crystals. *Crystal Research and Technology*, *46*(4), 327–330.

Kokh, K. A., Atuchin, V. V., Gavrilova, T. A., Kuratieva, N. V., Pervukhina, N. V., & Surovtsev, N. V. (2014). Microstructural and vibrational properties of PVT grown Sb_2Te_3 crystals. *Solid State Communications*, *177*, 16–19.

Lange, P. W. (1939). Ein Vergleich zwischen Bi_2Te_3 und Bi_2Te_2S. *Naturwissenschaften*, *27*(8), 133–134.

Lee, S., In, J., Yoo, Y., Jo, Y., Park, Y. C., Kim, H. J., et al. (2012). Single crystalline β-Ag_2Te nanowire as a new topological insulator. *Nano Letters*, *12*(8), 4194–4199.

Ma, X. H., Cho, K. H., & Sung, Y. M. (2014). Growth mechanism of vertically aligned SnSe nanosheets via physical vapour deposition. *CrystEngComm*, *16*(23), 5080–5086.

Nakajima, S. (1963). The crystal structure of $Bi_2Te_{3-x}Se_x$. *Journal of Physics and Chemistry of Solids*, *24*(3), 479–485.

Niesner, D., Fauster, T., Eremeev, S. V., Menshchikova, T. V., Koroteev, Y. M., Protogenov, A. P., et al. (2012). Unoccupied topological states on bismuth chalcogenides. *Physical Review B: Condensed Matter*, *86*(20), 205403.

Norimatsu, K., Hu, J., Goto, A., Igarashi, K., Sasagawa, T., & Nakamura, K. G. (2013). Coherent optical phonons in a Bi_2Se_3 single crystal measured via transient anisotropic reflectivity. *Solid State Communications*, *157*, 58–61.

Okamoto, H. (1994). The Bi–Se (bismuth–selenium) system. *Journal of Phase Equilibria*, *15*(2), 195–201.

Ozawa, T. C., & Kang, S. J. (2004). Balls&Sticks: Easy-to-use structure visualization and animation program. *Journal of Applied Crystallography*, *37*(4), 679.

Piacente, V., Scardala, P., & Ferro, D. (1992). Study of the vaporization behaviour of Sb_2S_3 and Sb_2Te_3 from their vapour pressure measurements. *Journal of Alloys and Compounds*, *178*(1), 101–115.

Roy, S., Meyerheim, H. L., Mohseni, K., Ernst, A., Otrokov, M. M., Vergniory, M. G., et al. (2014). Atomic relaxations at the (0 0 0 1) surface of Bi_2Se_3 single crystals and ultrathin films. *Physical Review B: Condensed Matter*, *90*(15), 155456.

Sawada, S., & Danielson, G. C. (1959). Domain structure of WO_3 single crystals. *Physical Review*, *113*(4), 1005–1008.

Semiletov, S. A., & Pinsker, Z. G. (1955). Electronographic investigation of the bismuth-selenium system. *Doklady Akademii Nauk SSSR*, *100*, 1079–1082 (in Russian)

Sheldrick, G. M. (1998). *SHELX-97, release 97-2*. Germany: University of Göttingen.

Shevtsov, Y. V., & Beizel, N. F. (2011). Pb distribution in multistep bismuth refining products. *Inorganic Materials*, *47*(2), 139–142.

Shu, H. W., Jaulmes, S., & Flahaut, J. (1988). Systeme As Ge Te: III. Eťude cristallographique d'une famille de compose's a modeles structuraux communs: β-As_2Te_3, As_4GeTe_7 et As_2GenTe_{3+n} ($n = 1–5$). *Journal of Solid State Chemistry*, *74*(2), 277–286.

Vergniory, M. G., Otrokov, M. M., Thonig, D., Hoffmann, M., Maznichenko, I. V., Geilhufe, M., et al. (2014). Exchange interaction and its tuning in magnetic binary chalcogenides. *Physical Review B: Condensed Matter*, *89*(16), 165202.

Voutsas, G. P., Papazoglou, A. G., Rentzeperis, P. J., & Siapkas, D. (1985). The crystal structure of antimony selenide, Sb_2Se_3. *Zeitschrift für Kristallographie-Crystalline Materials*, *171*(1–4), 261–268.

Yang, S., Kang, J., Yue, Q., & Yao, K. (2014). Vapor phase growth and imaging stacking order of bilayer molybdenum disulfide. *The Journal of Physical Chemistry C*, *118*(17), 9203–9208.

Zhang, H., Liu, C. X., Qi, X. L., Dai, X., Fang, Z., & Zhang, S. C. (2009). Topological insulators in Bi_2Se_3, Bi_2Te_3 and Sb_2Te_3 with a single Dirac cone on the surface. *Nature Physics*, *5*(6), 438–442.

Please cite this article in press as: Atuchin, V. V., et al. Physical vapor transport growth and morphology of Bi_2Se_3 microcrystals. *Particuology* (2016), http://dx.doi.org/10.1016/j.partic.2015.10.003